Use of Computational Fluid Dynamics for improving freeze-dryers design and understanding. Part 1: Modelling the lyophilisation chamber

A Method to Empirically Set the Coefficients of an Analytical Model of Battery Aging

Alberto Bocca
Dept. of Control and Computer Engineering
Politecnico di Torino
Torino, Italy
alberto.bocca@polito.it

***Abstract*—The increase of battery-powered devices and systems, from consumer electronics to electric vehicles, means that the reliability analysis of such systems concerns both energy cells and battery packs, as well as circuitry. For this reason, battery modeling has been one of most developed research areas during the last two decades. In this context, the Millner model, which is based on crack propagation theory, provides an accurate mathematical model for the analysis of the degradation (i.e., aging or capacity fading) of lithium-ion cells.**

In order to extend the application of the Millner model in a practical and simplified way, this work describes a method to empirically set the coefficients of this model by extracting these values from experimental data only published by the manufacturer and some researchers. When simulating an AMP20m1HD-A prismatic pouch cell at different working and operating conditions, the results show an accurate analysis of the capacity fading, with an error of generally less than 3%.

Keywords - **Battery modeling, capacity fading, estimation.**

I. Introduction

The remarkable increase of battery-powered systems has drawn attention to electrical energy sources in recent years, even for the development of hybrid batteries (e.g., lithium-ion cells with supercapacitors) and scavenging devices (i.e., energy harvesting). In general, a user wants to extend the battery life as much as possible after purchasing a new device of consumer electronics (e.g., smartphone) or a power system (e.g., electric vehicle). As a result, many people have complained about the issue of the battery degradation of these products over time. The main reason is the reduction of usable battery capacity due to (i) "calendar aging" and (ii) cycle life [1]. The first effect concerns both reversible and irreversible self-discharge over time [2], which limits the maximum number of years of operation. Furthermore, storage temperature affects calendar aging. The second effect regarding the number of cycles, depends on both the working conditions (e.g., current rate) and operating conditions (e.g., temperature) of each charge-discharge cycle of a secondary (i.e., rechargeable) battery. Thus, an electronic designer must consider both the electrical battery cells and circuitry to analyze the reliability of any such system.

This work describes a practical method for the estimation of the parameters of an extended version of the Millner mathematical model [3], which was originally proposed for the aging analysis of a specific 26650 $LiFePO_4$ cylindrical cell [4]. The proposed methodology allows the adoption of this model for various lithium-based battery cells through the extraction of the model coefficients from product data only. An example application is provided for the AMP20m1HD-A pouch cell [5].

The paper is organized as follows: Section II provides an overview of background and related works regarding battery modeling, whereas Section III explains the proposed empirical method for the estimation of the parameters of the analytical model here considered. Finally, Section IV reports the results, and Section V draws some conclusions.

II. Background and Related Work

In the literature, the state-of-health (SOH) of a battery is a typical parameter related to the actual total energy capacity of an aged battery with respect to the nominal capacity of a fresh one. In this context, the energy is evaluated by considering the *capacity C* [Ah] of a battery as a correlated unit of reference. Although there is still not a standard definition of SOH in industry [6], it is generally described by the following expression:

$$SOH = \frac{C_{aged}}{C_{nom}} = 1 - \frac{C_{fade}}{C_{nom}} \tag{1}$$

where C_{aged} and C_{nom} are the aged capacity and the nominal capacity, respectively [7], and C_{fade} is the irreversible capacity loss. At the beginning of battery life, SOH=1 whereas end of life is usually defined for SOH=0.8 (or 80%), that is, after a normalized C_{fade} of 20% [6]. In general, a common method for estimating SOH is by measuring the internal equivalent DC resistance (less accurate) or AC impedance (more accurate but more challenging and expensive) [8]. However, the increasing of the internal resistance of a battery is not always related to capacity fade, that is, their relationship is not always well correlated [9]. Furthermore, C_{fade} originates from various internal complicated chemical and electrochemical processes which cannot be considered independently. For example, since the value of the internal resistance affects the temperature of a battery during charge/discharge cycles, it also impacts the capacity fade [10]. The description of all these processes is beyond the scope of this work. Nevertheless, basic knowledge is provided in order to explain the motivation of the methodology presented here.

The modeling of C_{fade} is generally based on mathematical models, which include electrochemical processes (e.g., [11], [12]), and equivalent electrical circuits (e.g., [13]). Electrochemical models include complex governing equations [14] whereas compact mathematical models are simple, although less accurate [15]. From a system-level analysis, the key parameters affecting C_{fade} are the following:

- **Temperature (T)**. The relation between battery degradation and temperature is typically described by an Arrhenius type function [16].
- **Depth-of-Discharge (DOD)**. This is the difference in the battery state-of-charge (SOC), which is the percentage of the total capacity still available during the discharge phase in a runtime. Therefore, a 100% DOD means that a fully charged battery has been fully discharged.
- **Charge/Discharge Current**. Although both charge and discharge currents affect aging, the charge current is usually predominant when analyzing the same current (absolute value) in both charging and discharging phases [17].
- **Number of cycles**. The correlation between C_{fade} and the number of cycles actually depends on the aforementioned key parameters, that is, on both operating and working conditions.
- **Average SOC**. From experimental data, the average SOC of a battery affects aging over time [18]. For this reason, some charge protocols can be programmed to fully charge a battery just before using the device, instead of starting an "as soon as possible" charging phase, with the consequence often of keeping the battery at SOC=100% for a long time [19].

All these factors influence aging in a directly proportional manner, and allow system-level aging models instead of complex models based on chemical and structural analysis.

Based on product data analysis, which has recently become a rather common technique in battery modeling [13], this work provides a practical method for populating an analytical aging model including all the aforementioned key parameters.

III. Scenario and Method

The Millner model for the analysis of battery aging was originally defined for an ANR26650 Nanophosphate® lithium iron phosphate ($LiFePO_4$ or LFP) battery [3]. This mathematical model was extended in [17] for the analysis of battery life degradation ($Life$) also due to charging, as follows:

$$Life(m) = Life_{_{Millner}} \cdot e^{(K_{ic} \cdot I_c + K_{id} \cdot I_d)} \qquad (2)$$

In (2), $Life_{_{Millner}}$ is the life degradation as defined by Millner [3]; the basic equations of that model are reported in the Appendix for the sake of completeness of this work. In the same equation, I_c and I_d are the charging current and discharging current, respectively, at cycle m; they are given in C-rate [h^{-1}], which is a normalized form of the battery current [A] with respect to the nominal capacity [Ah]. For example, 1C/-2C means to fully charge a battery (from 0 to 100% SOC) in one hour, and to fully deplete it in half an hour. However, in (2) both I_c and I_d are given in absolute values. K_{ic} and K_{id} are two coefficients, which are extracted from a logarithmic expression reported in a generalized form in (3), and define the increase in charge current I_c and discharge current I_d, respectively, which leads to double the irreversible capacity loss of the cell.

$$e^{K_{ix} \cdot \Delta I_x} = 2 \qquad \Rightarrow \qquad K_{ix} = ln(2)/\Delta I_x \qquad (3)$$

For an empirical extraction of each coefficient value, two plots regarding the capacity fading of the cell under test are necessary: only one parameter (i.e, I_c or I_d) should change. Similarly, this empirical method should be followed also for the other coefficients of the Millner model: T_{fact}, K_{ex}, K_{SOC} and K_{co}; they refer to the following key factors: temperature, DOD, average SOC (SOC_{avg}) and energy throughput, respectively. Although K_{SOC} was originally taken from [20], K_{ex} and K_{co} were extracted empirically in order to fit the experimental data regarding life degradation. In this work, these parameters are also extracted in a practical way, by analyzing some published experimental data and considering SOC_{avg} around 50-65% and DOD$\geq$65%.

By following this method, an electronic designer does not need expensive equipment for the analysis of the response of a battery cell that cycles in a specific application, as this model is sufficiently accurate for the purpose of a system-level simulation of battery life cycle. The only drawback is that this model requires the definition of all the coefficients related to the key factors in order to obtain reliable results. In Section IV, a more comprehensive explanation is provided, as it reports a real application of the proposed method.

Finally, the SOH of a battery cell after M cycles is then given by firstly adding up the degradation of each single cycle m and then subtracting this value to 1, as reported in (4).

$$SOH(M) = 1 - \sum_{m=1}^{M} Life(m) \qquad (4)$$

IV. Results

The capacity loss of the A123 Systems AMP20m1HD-A Nanophosphate® pouch cell [5] was analyzed through the proposed aging model as described in Section III. The specifications of this cell are reported in Table I.

TABLE I
20Ah prismatic pouch cell specifications [5].

Dimensions	7.25 x 160 x 227 mm
Weight	496 g
Capacity (min)	19.5 Ah
Energy content (nom)	65 Wh
Discharge power (nom)	1200 W
Voltage (nom)	3.3 V
Specific power (nom)	2400 W/kg
Specific energy (nom)	131 Wh/kg
Energy density	247 Wh/L
Operating temperature range	-30°C to 55°C
Storage temperature range	-40°C to 60°C

Similar to the ANR26650$m1$ cylindrical cell by A123 Systems (this cell is nowadays manufactured by Lithium Werks), the AMP20m1HD-A pouch cell also has Nanophosphate as cathode active material. However, the coefficient values of the aging models of these two cells are generally different, as shown hereafter. Nevertheless, this work considers the same calendar life of 15 years.

A. Capacity fading at constant current

Firstly, validation is carried out through the simulation of the model at various operating conditions and constant charge and discharge currents, and the subsequent comparison of the results with the experimental data. The latter are provided in the product documentation [21], [22] or by some researchers [9], [23].

TABLE II
COEFFICIENT VALUES OF THE AGING MODEL.

K_{co}	K_{ex}	K_{SOC}	K_T	K_{ic}	K_{id}
$1.350E^{-5}$	1.5	0.603800	$5.332E^{-2}$	0.192541	0.099021

Table II reports the coefficients of the model for the battery cell under test. K_{co} and K_{ex} are battery-specific coefficients; they refer to throughput and DOD, respectively. K_{SOC} refers to SOC$_{avg}$ and, therefore, the average voltage of the cell [3]. These coefficients were extracted empirically, especially using the data reported in [9], as they refer to the capacity fade of cells working at various DOD levels and average SOC levels. K_T was extracted similarly to (3), but for temperature:

$$e^{K_T \cdot \Delta T} = 2 \qquad \Rightarrow \qquad K_T = ln(2)/\Delta T \tag{5}$$

In fact, K_T (originally named T_{fact}) is related to the temperature difference (i.e., ΔT =13°C in this case), between the real operating condition and the reference temperature (i.e., 25°C), necessary to double the life degradation of the cell.

As some of the published data regarding capacity fade are originally plotted in charts against the corresponding energy throughput [kWh] on the abscissa, instead of number of cycles, all the simulation results are here reported in two different tables. In this way there is a true comparison of the estimates with the experimental data provided in the referred documents. Table III includes the tests for which the reference is the number of charge/discharge cycles of the battery, whereas Table IV includes the tests for which the reference is the total energy throughput [kWh]. Each of the test conditions (C-rate, DOD and T) are also provided in the documents cited in the first column of these tables. The experimental results, in column 6 of each table, were extracted from these documents, whereas the simulation results are given in the last column. As both the experimental and estimated values are already reported in a normalized form, the error is given by the absolute difference of them. The maximum error of 3% is noted in Table IV, for the test reported at rows three, whereas there is no error in Table III. The mean absolute error (MAE) of all the tests is 0.73.

TABLE III
ESTIMATION OF THE CAPACITY FADE OF THE AMP20m1HD-A CELL OPERATING AT VARIOUS CURRENT RATES AND TEMPERATURES

Ref.	C-rate	DOD [%]	T [°C]	Cycles	Normalized C	
					Exp.	*Est.*
[21]	1C/-1C	0 - 100	25	6000	0.77	0.78
[21]	1C/-1C	0 - 100	35	5000	0.70	0.70
[21]	1C/-1C	0 - 100	45	3000	0.71	0.71
[22]	1C/-2C	0 - 100	23	3000	0.89	0.89
[23]	2.5C/-1C	0 - 100	23	2500	0.79	0.79

TABLE IV
ESTIMATION OF THE CAPACITY FADE OF THE AMP20m1HD-A CELL OPERATING AT VARIOUS CHARGE RATES AND DODS

Ref.	C-rate	DOD [%]	T [°C]	Energy thr. [kWh]	Normalized C	
					Exp.	*Est.*
[21]	1C/-1C	0 - 100	23	350	0.91	0.90
[21]	3C/-1C	0 - 100	23	250	0.90	0.89
[21]	4C/-1C	0 - 100	23	290	0.88	0.85
[9]	1C/-1C	25 - 90	23	400	0.87	0.89
[9]	1C/-1C	35 - 100	23	275	0.92	0.90
[9]	1C/-1C	25 - 100	23	300	0.91	0.90

It is necessary to point out that Table III reports a mean value for the experimental data of the test at 45°C (row three), as the results in [21] slightly differ after testing two cells at the same working conditions, as reported by the manufacturer.

Fig. 1 reports the capacity fade of three AMP20m1HD-A cells cycling at various charge currents and a constant discharge current of 1C at T=23°C. Here, the experimental data are provided in [21].

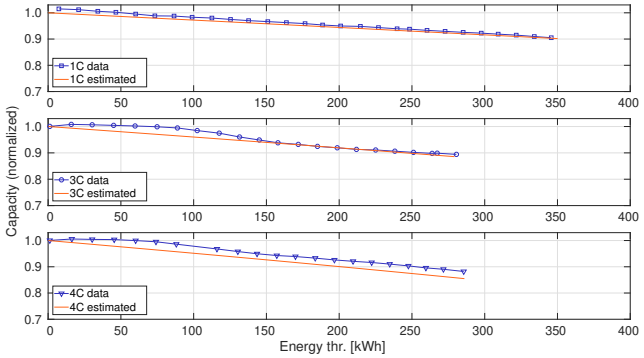

Fig. 1. Capacity vs. energy throughput: validation data for various charging rates @ T=23°C, I_d=-1C and DOD=100% [21].

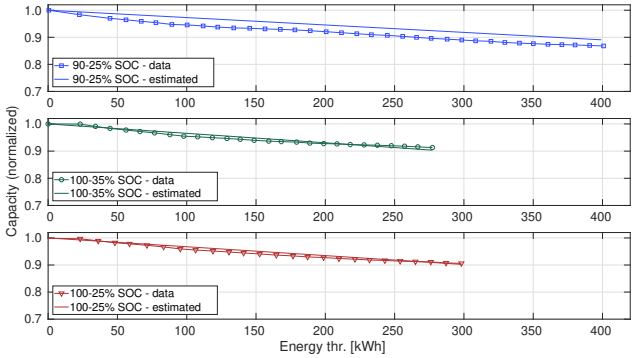

Fig. 2. Capacity vs. energy throughput: validation data for various DODs and average SOC @ T=23°C, I_c=1C and I_d=-1C [9].

Fig. 2 shows the experimental data provided in [9], and the estimated data from the model simulation regarding the capacity fade of three cells which cycle at different DODs or SOC_{avg}.

Fig. 3 reports a comparison of the estimated results with the experimental data of the capacity fade, as provided in [21], at different ambient temperatures and at the constant working conditions of 1C/-1C current rates and 100% DOD.

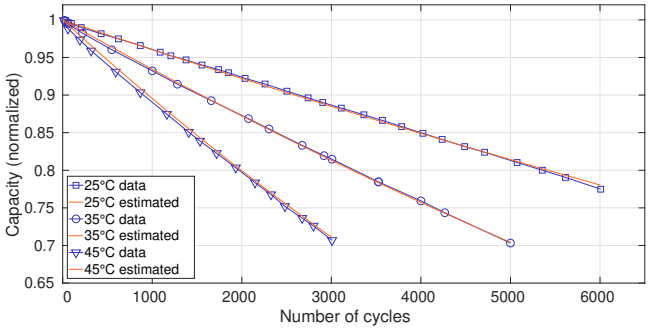

Fig. 3. Capacity vs. number of cycles at various temperatures @ I_c=1C and I_d=-1C and DOD=100% [21].

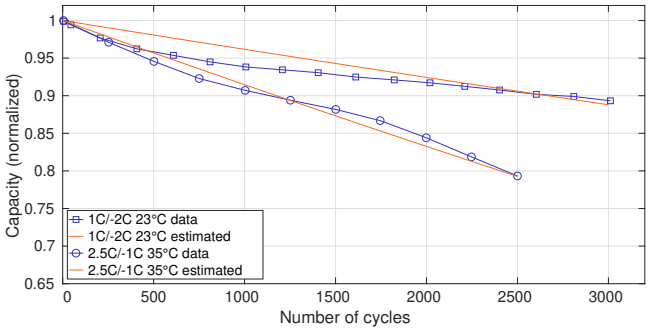

Fig. 4. Capacity vs. number of cycles @ DOD=100%: experimental data [22], [23].

Finally, Fig. 4 reports the validation of the model by comparing the simulation results to two different documents regarding the aging of the same type of battery under test [22], [23]. Indeed, the experimental data in [22] was also useful to extract K_{id}, when comparing the aging at I_d=2C to another plot for the aging of the battery under test at the same conditions but I_d=1C [21]. Nevertheless, the above figures show the effectiveness of the model after applying the proposed methodology for setting the coefficients of the aging parameters.

B. Capacity fading at a dynamic current profile

For a comprehensive validation of the proposed model, a further simulation is necessary for evaluating the capacity fade of the pouch cell under test when operating at a dynamic current profile. For this purpose, some experimental data were extracted from [24], in particular the characteristic $current\ vs.\ time$ for a test period of five hours, and the experimental results regarding 250 cycles at two different test temperatures: room temperature (rt) and 45°C. In this analysis, the SOC of the cell is always in a range from 0.1 to 0.9, in order to operate in the most common working conditions, and the current in a range from -1C to 1C.

Fig. 5 reports the simulation results regarding the capacity fading and the experimental results extracted from [24]. The error is about 0.5% at room temperature, which is considered in a range between 22-26°C, and 0.3% at 45 °C. These results confirm both the reliability and accuracy of the battery model for both constant and dynamic currents.

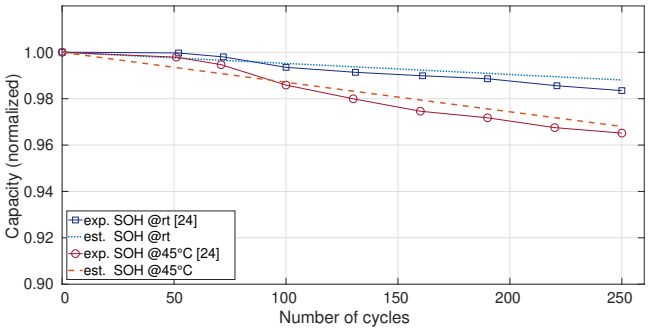

Fig. 5. Validation of the model for a dynamic charge/discharge current profile extracted from [24].

As high temperature is the primary factor of aging in LFP cells [24], it is obvious that in a pack with cells connected in series and parallel, the real temperature of each cell depends also on the position in the pack. For this reason, the SOH of these connected cells during cycle life may differ one from another. Furthermore, the capacity fade of each single cell is not the only contributor to total energy loss. In fact, the difference in lithium concentration in the anodes of these cells also affects the capacity fade of a pack [25]. As a consequence, the aging analysis for high-capacity batteries, such as in the case of power applications, should require a further extension of the basic model; however, this is considered for a future work. Nevertheless, the proposed battery model may assist a designer for a true analysis of a cell for a specific battery-powered electronic device, after populating the model at system level through an empirical method.

V. Conclusion

This work described a method for generalizing the original Millner model for the analysis of the aging of lithium-based cells. The extraction of the model coefficients was empirically carried out from existing published data. Following this method, an accurate aging model for a system-level analysis can be generated by an electronic designer with lower effort and costs with respect to a direct analysis from testing.

For an AMP20m1HD-A pouch cell, the simulation results show an absolute error of between 0 and 3% with respect to the experimental data of capacity fading after various tests of thousands of cycles at different working and operating conditions.

REFERENCES

[1] R. Spotnitz, "Simulation of capacity fade in lithium-ion batteries," Journal of Power Sources, vol. 113, no. 1, pp. 72–80, 2003.

[2] M. Kassem, J. Bernard, R. Revel, S. Pelissier, F. Duclaud, and C. Delacourt, "Calendar aging of a graphite/LiFePO4 cell," Journal of Power Sources, vol. 208, pp. 296–305, 2012.

[3] A. Millner, "Modeling lithium ion battery degradation in electric vehicles," in Proc. IEEE Conference on Innovative Technologies for an Efficient and Reliable Electricity Supply (CITRES), 2010, pp. 349–356.

[4] A123 Systems, Inc., "High Power Lithium Ion ANR26650m1 datasheet," 2006.

[5] A123 Systems Inc., "20Ah Prismatic Pouch Cell Nanophosphate Lithium-Ion," datasheet, 2015.

[6] L. Lu, X. Han, J. Li, J. Hua, and M. Ouyang, "A review on the key issues for lithium-ion battery management in electric vehicles," Journal of Power Sources, vol. 226, pp. 272–288, 2013.

[7] M. Coleman, W. G. Hurley, and C. K. Lee, "An improved battery characterization method using a two-pulse load test," IEEE Transactions on Energy Conversion, vol. 23, no. 2, pp. 708–713, June 2008.

[8] W. Waag, C. Fleischer, and D. U. Sauer, "Critical review of the methods for monitoring of lithium-ion batteries in electric and hybrid vehicles," Journal of Power Sources, vol. 258, pp. 321–339, 2014.

[9] M. T. Lawder, B. Suthar, P. W. Northrop, S. De, C. M. Hoff, O. Leitermann, M. L. Crow, S. Santhanagopalan, and V. R. Subramanian, ' 'Battery energy storage system (BESS) and battery management system (BMS) for grid-scale applications," Proceedings of the IEEE, vol. 102, no. 6, pp. 1014–1030, June 2014.

[10] N. Omar et al., "Lithium iron phosphate based battery — Assessment of the aging parameters and development of cycle life model," Applied Energy, vol. 113, pp. 1575–1585, 2014.

[11] K. Uddin, S. Perera, W. Widanage, L. Somerville, and J. Marco, "Characterising lithium-ion battery degradation through the identification and tracking of electrochemical battery model parameters," Batteries, vol. 2, no. 2, 13, pp. 1–17, 2016.

[12] P. Ramadass, B. Haran, R. White, and B. N. Popov, "Mathematical modeling of the capacity fade of Li-ion cells," Journal of Power Sources, vol. 123, no. 2, pp. 230–240, 2003.

[13] M. Petricca, D. Shin, A. Bocca, A. Macii, E. Macii, and M. Poncino, "Automated generation of battery aging models from datasheets," in Proc. 32nd IEEE International Conference on Computer Design (ICCD), 2014, pp. 483–488.

[14] V. Ramadesigan, K. Chen, N. A. Burns, V. Boovaragavan, R. D. Braatz, and V. R. Subramanian, "Parameter estimation and capacity fade analysis of lithium-ion batteries using reformulated models," Journal of the Electrochemical Society, vol. 158, no. 9, pp. A1048–A1054, 2011.

[15] A. Bocca, A. Sassone, D. Shin, A. Macii, E. Macii, and M. Poncino, "An equation-based battery cycle life model for various battery chemistries," in Proc. 23rd IFIP/IEEE International Conference on Very Large Scale Integration (VLSI-SoC), 2015, pp. 57–62.

[16] T. Yuksel and J. Michalek, "Evaluation of the effects of thermal management on battery life in plug-in hybrid electric vehicles," in Battery Congress, April 2012.

[17] A. Bocca, A. Sassone, A. Macii, E. Macii, and M. Poncino, "An aging aware battery charge scheme for mobile devices exploiting plug-in time patterns," in Proc. 33rd IEEE International Conference on Computer Design (ICCD), 2015, pp. 407–410.

[18] J. Vetter, P. Novak, M. R. Wagner, C. Veit, K. C. Moller, J. O. Besenhard, M. Winter, M. Wohlfahrt-Mehrens, and A. Hammouche, "Ageing mechanisms in lithium-ion batteries," Journal of Power Sources, vol. 147, no. 1-2, pp. 269–281, 2005.

[19] Y. Chen, A. Bocca, A. Macii, E. Macii, and M. Poncino, "A Li-ion battery charge protocol with optimal aging-quality of service trade-off," in Proceedings of the 2016 International Symposium on Low Power Electronics and Design (ISLPED), 2016, pp. 40–45.

[20] S. B. Peterson, J. Apt, and J. Whitacre, "Lithium-ion battery cell degradation resulting from realistic vehicle and vehicle-to-grid utilization," Journal of Power Sources, vol. 195, no. 8, pp. 2385–2392, 2010.

[21] A123 Systems Inc., "Battery Pack Design, Validation, and Assembly Guide using A123 Systems AMP20m1HD-A Nanophosphate Cells," 7 February 2014.

[22] A123 Systems Inc., "Nanophosphate® Basics: An Overview of the Structure, Properties and Benefits of A123 Systems' Proprietary Lithium Ion Battery Technology," 2013.

[23] S. Kukkonen et al., "Dimensioning a battery and thermal management system, case eBus," in ECV National Seminar, Lappenranta, Finland, 2015.

[24] V. Vega-Garita, A. Hanif, N. Narayan, L. Ramirez-Elizondo, and P. Bauer, "Selecting a suitable battery technology for the photovoltaic battery integrated module," Journal of Power Sources, vol. 438, p. 227011, 2019.

[25] Y. Zheng, M. Ouyang, L. Lu, and J. Li, "Understanding aging mechanisms in lithium-ion battery packs: From cell capacity loss to pack capacity evolution," Journal of Power Sources, vol. 278, pp. 287–295, 2015.

APPENDIX

The fundamental equations of the Millner model for lithium-ion batteries [3] are reported here.

$$Life_1 = K_{co} \cdot N \cdot e^{(SOC_{dev}-1)/(K_{ex} \cdot \frac{T_{nabs}}{T_a})} + 0.2 \cdot \frac{t_{cycle}}{t_{life}} \quad (6)$$

$$Life_2 = Life_1 \cdot e^{K_{soc} \cdot ((SOCavg-0.5)/0.25)} \cdot (1-L) \quad (7)$$

$Life_1$ and $Life_2$ are the life degradation in a cycle due to (i) SOC swing and throughput, and (ii) SOC_{avg} and the reduction of lithium ion concentration, respectively.

The life degradation of a cell after a generic cycle m, including the thermal effects, is then given by the following equation:

$$Life(m) = Life_2 \cdot e^{T_{fact} \cdot (T - T_{nom}) \cdot \frac{T_{nabs}}{T_a}} \quad (8)$$

In (8), the term $Life$ refers to the term $Life_{Millner}$ in (2). Total life degradation L after M cycles is therefore given by:

$$L = \sum_{m=1}^{M} Life(m) \quad (9)$$

The parameters of these equations, which were not defined in the previous sections, are reported in Table V.

TABLE V
LIST OF THE PARAMETERS

Acronym	Definition
N	number of throughput cycles
SOC_{dev}	SOC deviation, from 0 to 1.0, in a cycle m
T_{fact}	this is K_T as defined in (5)
T	the temperature of the battery [°C]
T_a	this is T in Kelvin degrees
T_{nom}	reference temperature (i.e., 25°C)
T_{nabs}	reference temperature in Kelvin degrees
t_{cycle}	time of a cycle [s]
t_{life}	calendar life [s] to 80% capacity at 25°C and 50% SOC